ORIGINAL ARTICLE



WILEY

Long non-coding RNA EWSAT1 promoted metastasis and actin cytoskeleton changes via miR-24-3p sponging in osteosarcoma

Dewei Shen¹ | Yize Liu¹ | Yuexin Liu² | Tao Wang¹ | Lin Yuan³ | Xuyang Huang⁴ | Yong Wang^{1,5}

¹4th Department of Orthopaedic Surgery, Central Hospital affiliated to Shenyang Medical College, Shenyang, China

²School of Basic Medical Sciences, Shenyang Medical College, Shenyang, China

 $^32^{nd}$ Department of Orthopaedic Surgery, Second Affiliated Hospital of Shenyang Medical College, Shenyang, China

⁴2nd Department of Neurology, Central Hospital affiliated to Shenyang Medical College, Shenyang, China

⁵Central Laboratory, Central Hospital Affiliated to Shenyang Medical College, Shenyang, China

Correspondence

Yong Wang, Central Laboratory/4th Department of Orthopedic Surgery, Central Hospital Affiliated to Shenyang Medical College, No. 5, South Seven West Road, Tiexi District, Shenyang, Liaoning 110024, China.

Email: wy_landy1116@163.com

Funding information

SMC General Science Foundation, Grant/ Award Number: 20182034; Youth Talent Support Program of Liaoning Province, Grant/Award Number: XLYC1907011; SMC Students' scientific research projects, Grant/Award Number: 20189021; Key R&D Program of Liaoning Province, Grant/Award Number: 2018225014; Higher Institute Program Foundation for the Innovative Talents of Liaoning Province, Grant/ Award Number: LR2017056; Technological innovation fund of Shenyang Technology Division, Grant/Award Number: 19-112-4-023 and RC19000; National Natural Science Foundation of China, Grant/Award Number: 81502333 and 81972522

Abstract

Non-coding RNAs are closely associated with tumorigenesis in multiple malignant tumours, including osteosarcoma (OS). Long non-coding RNA Ewing sarcoma-associated transcript 1 (EWSAT1) plays a role in metastasis, and actin cytoskeletal changes in OS remain unclear. In the current study, we showed that EWSAT1 expression was up-regulated in OS and that an elevation in the EWSAT1 expression level was correlated with poor prognosis in patients with OS. Functionally, we showed that knockdown of EWSAT1 suppressed migration and induced actin stress fibre degradation in MNNG/HOS and 143B cells. Moreover, we found that ROCK1 was a key downstream effector in EWSAT1-mediated cell migration and actin stress fibre changes. Furthermore, we demonstrated that ROCK1 and EWSAT1 shared a similar micro-RNA response element of microRNA-24-3p (miR-24-3p). Moreover, we verified that miR-24-3p suppressed ROCK1 and its mediated migration and actin stress fibres change by direct targeting. EWSAT1 promoted ROCK1-mediated migration and actin stress fibre formation through miR-24-3p sponging. Lastly, through an in vivo study, we demonstrated that EWSAT1 promoted lung metastasis in OS. According to the above-mentioned results, we suggest that EWSAT1 acts as an oncogene and that EWSAT1/miR-24-3p/ROCK1 axial could be a new target in the treatment of OS.

KEYWORDS

actin stress fibre formation, IncRNAEWSAT1, metastasis, miR-24-3p, osteosarcoma

Dewei Shen, Yize Liu and Yuexin Liu contributed equally to this work and should be listed as co-first authors.

This is an open access article under the terms of the Creative Commons Attribution License, which permits use, distribution and reproduction in any medium, provided the original work is properly cited.

© 2020 The Authors. Journal of Cellular and Molecular Medicine published by Foundation for Cellular and Molecular Medicine and John Wiley & Sons Ltd

J Cell Mol Med. 2020:00:1-13. wileyonlinelibrary.com/journal/jcmm

1 | INTRODUCTION

As the most prevalent primary sarcoma in young adolescence, osteo-sarcoma (OS) commonly develops at the metaphysis of long bones and produces a bone or osteoid. The highest aggressive phenotypes and fast growth and early stage of pulmonary metastasis are the main factors for the unfavourable prognosis of OS. According to an epidemiological study, approximately 20% of patients had pulmonary metastasis in their first clinical visit. Although a combined treatment, involving tumorectomy and chemotherapy, significantly improves the survival rate of patients with OS, the survival period of the involved individuals who present with lung metastasis remains non-optimistic. Although a combined treatment, involving tumorectomy and chemotherapy, significantly improves the survival rate of patients with OS, the survival period of the involved individuals who present with lung metastasis remains non-optimistic. Therefore, there is an urgent need for determining available metastatic molecules and identifying their underlying mechanisms in OS.

Long non-coding RNAs (IncRNAs), with a length of >200 nucleotides, belong to a class of non-protein-coding transcriptions and are extensively involved in a crowd of cell biological events. LncRNAs may function as scaffolds or guide in regulating interactions between proteins and genes and can also act as enhancers to modulate transcription of their targets. 5-7 EWSAT1, also named LINC00277, was first reported as an oncogenic transcription in Ewing sarcoma.⁸ Presently, related studies on EWSAT1 are rare. Through a protein array analysis and RNA immunoprecipitation assay, Margues reported that EWSAT1 regulated gene expression partially through interaction with the heterogeneous nuclear ribonucleoprotein.8 Sun reported that EWSAT1 positively regulated IncRNA MEG3 expression at the transcriptional level and that EWSAT1 promoted OS cell growth and metastasis.9 It is well known that IncRNAs can also function by acting through microRNA (miRNA) sponging or competitive endogenous RNA (ceRNA), which was first proposed by Leonardo Salmena in 2011. 10 The CeRNA hypothesis is that all types of RNA transcripts communicate through a new "language" mediated by miRNA-binding sites ("microRNA response elements," or "MREs"). 10 Our previous studies revealed that IncRNAs, including taurine-up-regulated gene 1 (TUG1), metastasis-associated lung adenocarcinoma transcript 1 (MALAT1), differentiation antagonizing non-protein coding RNA (DANCR) and nuclear-enriched abundant transcript 1 (NEAT1) exerted their oncogenic functions in OS, colorectal cancer and ovarian cancer through the ceRNA mechanism. 11-15 Here, we considered EWSAT1, a new IncRNA, as a research point and illustrated the oncogenic role of EWSAT in OS, especially in metastasis and actin stress fibre formation.

2 | MATERIALS AND METHODS

2.1 | Patients and tissue samples

We collected 50 OS tissue specimens and paired paratumour tissue specimens during tumorectomy at Liaoning Cancer Hospital & Institute between January 2015 and January 2018. All cases were diagnosed as OS according to the clear histologic diagnosis of OS and staged according to the TNM classification of the International Union Against Cancer. Written informed consent was provided by the patients whose

tissues were used in this study. The Institute Research Medical Ethics Committee of Central Hospital Affiliated to Shenyang Medical College and Institute Research Medical Ethics Committee of Liaoning Cancer Hospital & Institute approved this study.

2.2 | Cell culture

The human osteoblast cell line hFOB 1.19 was cultured in Dulbecco's modified Eagle's medium (DMEM)/F12 (Gibco). The human OS cell lines MG-63, U2OS, MNNG/HOS and 143B were cultured in DMEM (Gibco). HEK-293 cells were cultured in MEM (Gibco). All culture media were supplemented with 10% (v/v) foetal bovine serum (FBS; Sigma), 100 IU/mL penicillin (Baomanbio) and 100 mg/mL streptomycin (Baomanbio). All OS cell lines and HEK-293 were incubated at 37°C, while hFOB 1.19 was cultured at 34°C in a humidified atmosphere containing 5% CO₂. The cultured cells were passaged when they grew to 80% confluence.

2.3 | Reverse transcription and quantitative realtime PCR

The procedure was conducted as previously described.¹³ Total RNAs were isolated using TRIzol reagent (Invitrogen). A Takara RNA PCR kit (Takara) was applied to synthesize cDNA according to the manufacturer's protocol. PCR assays containing SYBR Premix Ex Taq II (Takara) were performed according to the manufacturer's manual. U6 small nuclear RNA and GAPDH were used as internal controls. Primer sequences, as presented in Table 1, were synthesized by RiboBio Co., Ltd.

2.4 | Oligonucleotide and plasmid transfection

Effective siRNA oligonucleotides that targeted EWSAT1 (1# si-EWSAT1 and 2# si-EWSAT1) and the corresponding control siRNA (si-con), miR-24-3p oligonucleotides including miR-24-3p mimics and mimic control, miR-24-3p inhibitors and inhibitor control were synthesized by RiboBio. Oligonucleotide sequences are also shown in Table 1. EWSAT1 overexpression plasmids (oe-EWSAT1) and ROCK1 overexpression plasmids (oe-ROCK1) were chemically synthetized by GenePharma. When MNNG/HOS and 143B cells reached 70-80% confluence, the aforementioned oligonucleotides and plasmids were transfected to the cultured OS cells using Lipofectamine 3000 (Invitrogen) according to the manufacturer's instructions. Y-27632 dihydrochloride (Abcam) was used as a selective ROCK1 blocker.

2.5 | In situ hybridization (ISH) assay

The procedure of ISH and IHC was performed as previously described. ¹⁶ Briefly, specific probes targeting EWSAT1 and miR-24-3p were purchased from Boster Bio Co., Ltd. The probes were added

TABLE 1 Primer sequences used in the present research

EWSAT1-F for PCR AGAAAGGCTGTGACAGCAT EWSAT1-R for PCR TCCCTCCTTCCACCTTCC ROCK1-F for PCR AGGAAGGCGGACATATTAGTCCCT ROCK1-R for PCR AGGAAGGCGGACATATTAGTCCCT ROCK1-R for PCR AGACGATAGTTGGGTC CCGGC GAPDH-F for PCR GCACCGTCAAGGCTGAGAAC GAPDH-R for PCR TGGTGAAGACGCCAGTGGA miR-24-3p-F for PCR GGGTGGCTCAGTCAGCAG miR-24-3p-R for PCR GGGTCAGTCAGAGAC miR-335-5p-F for PCR GGGTCAAGAGCAATAACGAA miR-335-5p-R for CAGTGCGTGTCGTGGAGT PCR miR-144-3p-F for PCR GGGTACAGTATAGATGA miR-144-3p-R for CAGTGCGTGTCGTGGAGT PCR U6-F for PCR CTCGCTTCGGCAGCACA U6-R for PCR ACGCTTCACGAATTTGCGT EWSAT1-01 siRNA GCACAGCATCCTTGCTCTA EWSAT1-02 siRNA GGAGTTATCAGAGCCA miR-24-3p mimics TGGCTCAGTGACCA CTGTTCCTGCTGAACTGAGCCA CTGTTCCTGCTGAACTGAGCCA		·
EWSAT1-R for PCR ROCK1-F for PCR AGGAAGGCGGACATATTAGTCCCT ROCK1-R for PCR AGACGATAGTTGGGTC CCGGC GAPDH-F for PCR GCACCGTCAAGGCTGAGAAC GAPDH-R for PCR TGGTGAAGACGCCAGTGGA miR-24-3p-F for PCR GGGTGGCTCAGTTCAGCAG miR-335-5p-F for PCR GGGTCAAGAGCAATAACGAA miR-335-5p-R for PCR miR-144-3p-F for PCR GGGTACAGTATAGATGA miR-144-3p-R for PCR U6-F for PCR CTCGCTTCGGCAGCACA U6-R for PCR AACGCTTCACGAATTTGCGT EWSAT1-01 siRNA GGAGTTATCTGGGTATCAA miR-24-3p mimics TGGCTCAGTTCAGCAGGAACAG TGGCTCAGTATCAAA TGGCTCAGTATCAAA TGGCTCAGTATCAAA TGGCTCAGTATCAAA TGGCTCAGTATCAAA TGGCTCAGTTCAGCAGGAACAG TGGCTCAGTTCACCAGGAACAG TGGCTCAGTTCAGCAGGAACAG TGGCTCAGTTCAGCAGGAACAG TGGCTCAGTTCAGCAGGAACAG	Gene	Sequences of primers used
ROCK1-F for PCR AGGAAGGCGGACATATTAGTCCCT ROCK1-R for PCR AGACGATAGTTGGGTC CCGGC GAPDH-F for PCR GCACCGTCAAGGCTGAGAAC GAPDH-R for PCR TGGTGAAGACGCCAGTGGA miR-24-3p-F for PCR GGGTGGCTCAGTTCAGCAG miR-24-3p-R for PCR CAGTGCGTGTCGTGGAGT miR-335-5p-F for PCR GGGTCAAGACAATAACGAA miR-335-5p-R for CAGTGCGTGTCGTGGAGT PCR miR-144-3p-F for PCR GGGTACAGTATAGATGA miR-144-3p-R for CAGTGCGTGTCGTGGAGT PCR U6-F for PCR CTCGCTTCGGCAGCACA U6-R for PCR AACGCTTCACGAATTTGCGT EWSAT1-01 siRNA GCACAGCATCCTTGCTCTA EWSAT1-02 siRNA GGAGTTATCTGGGTATCAA miR-24-3p mimics TGGCTCAGTTCAGCAGGAACAG	EWSAT1-F for PCR	AGAAAGGGCTGTGACAGCAT
ROCK1-R for PCR AGACGATAGTTGGGTC CCGGC GAPDH-F for PCR GCACCGTCAAGGCTGAGAAC GAPDH-R for PCR TGGTGAAGACGCCAGTGGA miR-24-3p-F for PCR GGGTGGCTCAGTTCAGCAG miR-24-3p-R for PCR CAGTGCGTGTCGTGGAGT miR-335-5p-F for PCR GGGTCAAGAGCAATAACGAA miR-335-5p-R for CAGTGCGTGTCGTGGAGT PCR miR-144-3p-F for PCR GGGTACAGTATAGATGA miR-144-3p-R for CAGTGCGTGTCGTGGAGT PCR U6-F for PCR CTCGCTTCGGCAGCACA U6-R for PCR AACGCTTCACGAATTTGCGT EWSAT1-01 siRNA GCACAGCATCCTTGCTCTA EWSAT1-02 siRNA GGAGTTATCTGGGTATCAA miR-24-3p mimics TGGCTCAGTAGCAGGAACAG	EWSAT1-R for PCR	TCCCTCCTTCCACCTTCC
GAPDH-F for PCR GCACCGTCAAGGCTGAGAAC GAPDH-R for PCR TGGTGAAGACGCCAGTGGA miR-24-3p-F for PCR GGGTGGCTCAGTTCAGCAG miR-24-3p-R for PCR CAGTGCGTGTCGTGGAGT miR-335-5p-F for PCR GGGTCAAGAGCAATAACGAA miR-335-5p-R for PCR miR-144-3p-F for PCR GGGTACAGTATAGATGA miR-144-3p-R for PCR U6-F for PCR CTCGCTTCGGCAGCACA U6-R for PCR AACGCTTCACGAATTTGCGT EWSAT1-01 siRNA GCACAGCATCCTTGCTCTA EWSAT1-02 siRNA GGAGTTATCTGGGTATCAA miR-24-3p mimics TGGCTCAGTTCAGCAGGAACAG	ROCK1-F for PCR	AGGAAGGCGGACATATTAGTCCCT
GAPDH-R for PCR miR-24-3p-F for PCR GGGTGGCTCAGTTCAGCAG miR-24-3p-R for PCR CAGTGCGTGTCGTGGAGT miR-335-5p-F for PCR GGGTCAAGAGCAATAACGAA miR-335-5p-R for PCR miR-144-3p-F for PCR GGGTACAGTATAGATGA miR-144-3p-R for PCR U6-F for PCR CTCGCTTCGGCAGCACA U6-R for PCR AACGCTTCACGAATTTGCGT EWSAT1-01 siRNA GGAGTTATCTGGGTATCAA miR-24-3p mimics TGGCTCAGTTCAGCAGGAACAG TGGCTCAGTATCAGCAGGAACAG TGGCTCAGTATCAGCAGGAACAG TGGCTCAGTTCAGCAGGAACAG TGGCTCAGTTCAGCAGGAACAG	ROCK1-R for PCR	AGACGATAGTTGGGTC CCGGC
miR-24-3p-F for PCR GGGTGGCTCAGTTCAGCAG miR-24-3p-R for PCR CAGTGCGTGTGGAGT miR-335-5p-F for PCR GGGTCAAGAGCAATAACGAA miR-335-5p-R for CAGTGCGTGTCGTGGAGT PCR miR-144-3p-F for PCR GGGTACAGTATAGATGA miR-144-3p-R for CAGTGCGTGTCGTGGAGT PCR U6-F for PCR CTCGCTTCGGCAGCACA U6-R for PCR AACGCTTCACGAATTTGCGT EWSAT1-01 siRNA GCACAGCATCCTTGCTCTA EWSAT1-02 siRNA GGAGTTATCTGGGTATCAA miR-24-3p mimics TGGCTCAGTAGAGTACAGGAACAG	GAPDH-F for PCR	GCACCGTCAAGGCTGAGAAC
miR-24-3p-R for PCR CAGTGCGTGTCGTGGAGT miR-335-5p-F for PCR GGGTCAAGAGCAATAACGAA miR-335-5p-R for CAGTGCGTGTCGTGGAGT PCR miR-144-3p-F for PCR GGGTACAGTATAGATGA miR-144-3p-R for CAGTGCGTGTCGTGGAGT PCR U6-F for PCR CTCGCTTCGGCAGCACA U6-R for PCR AACGCTTCACGAATTTGCGT EWSAT1-01 siRNA GCACAGCATCCTTGCTCTA EWSAT1-02 siRNA GGAGTTATCTGGGTATCAA miR-24-3p mimics TGGCTCAGTATCAGCAGGAACAG	GAPDH-R for PCR	TGGTGAAGACGCCAGTGGA
miR-335-5p-F for PCR GGGTCAAGAGCAATAACGAA miR-335-5p-R for CAGTGCGTGTCGTGGAGT PCR miR-144-3p-F for PCR GGGTACAGTATAGATGA miR-144-3p-R for CAGTGCGTGTCGTGGAGT PCR U6-F for PCR CTCGCTTCGGCAGCACA U6-R for PCR AACGCTTCACGAATTTGCGT EWSAT1-01 siRNA GCACAGCATCCTTGCTCTA EWSAT1-02 siRNA GGAGTTATCTGGGTATCAA miR-24-3p mimics TGGCTCAGTAGAACAG	miR-24-3p-F for PCR	GGGTGGCTCAGTTCAGCAG
miR-335-5p-R for PCR miR-144-3p-F for PCR GGGTACAGTATAGATGA miR-144-3p-R for CAGTGCGTGTCGTGGAGT PCR U6-F for PCR CTCGCTTCGGCAGCACA U6-R for PCR AACGCTTCACGAATTTGCGT EWSAT1-01 siRNA GCACAGCATCCTTGCTCTA EWSAT1-02 siRNA GGAGTTATCTGGGTATCAA miR-24-3p mimics TGGCTCAGTTCAGCAGGAACAG	miR-24-3p-R for PCR	CAGTGCGTGTGGAGT
PCR miR-144-3p-F for PCR GGGTACAGTATAGATGA miR-144-3p-R for CAGTGCGTGTCGTGGAGT PCR U6-F for PCR CTCGCTTCGGCAGCACA U6-R for PCR AACGCTTCACGAATTTGCGT EWSAT1-01 siRNA GCACAGCATCCTTGCTCTA EWSAT1-02 siRNA GGAGTTATCTGGGTATCAA miR-24-3p mimics TGGCTCAGTTCAGCAGGAACAG	miR-335-5p-F for PCR	GGGTCAAGAGCAATAACGAA
miR-144-3p-R for PCR U6-F for PCR CTCGCTTCGGCAGCACA U6-R for PCR AACGCTTCACGAATTTGCGT EWSAT1-01 siRNA GCACAGCATCCTTGCTCTA EWSAT1-02 siRNA GGAGTTATCTGGGTATCAA miR-24-3p mimics TGGCTCAGTTCAGCAGGAACAG		CAGTGCGTGTCGTGGAGT
PCR U6-F for PCR CTCGCTTCGGCAGCACA U6-R for PCR AACGCTTCACGAATTTGCGT EWSAT1-01 siRNA GCACAGCATCCTTGCTCTA EWSAT1-02 siRNA GGAGTTATCTGGGTATCAA miR-24-3p mimics TGGCTCAGTTCAGCAGGAACAG	miR-144-3p-F for PCR	GGGTACAGTATAGATGA
U6-R for PCR AACGCTTCACGAATTTGCGT EWSAT1-01 siRNA GCACAGCATCCTTGCTCTA EWSAT1-02 siRNA GGAGTTATCTGGGTATCAA miR-24-3p mimics TGGCTCAGTTCAGCAGGAACAG	· ·	CAGTGCGTGTCGTGGAGT
EWSAT1-01 siRNA GCACAGCATCCTTGCTCTA EWSAT1-02 siRNA GGAGTTATCTGGGTATCAA miR-24-3p mimics TGGCTCAGTTCAGCAGGAACAG	U6-F for PCR	CTCGCTTCGGCAGCACA
EWSAT1-02 siRNA GGAGTTATCTGGGTATCAA miR-24-3p mimics TGGCTCAGTTCAGCAGGAACAG	U6-R for PCR	AACGCTTCACGAATTTGCGT
miR-24-3p mimics TGGCTCAGTTCAGCAGGAACAG	EWSAT1-01 siRNA	GCACAGCATCCTTGCTCTA
	EWSAT1-02 siRNA	GGAGTTATCTGGGTATCAA
miR-24-3p inhibitor CTGTTCCTGCTGAACTGAGCCA	miR-24-3p mimics	TGGCTCAGTTCAGCAGGAACAG
	miR-24-3p inhibitor	CTGTTCCTGCTGAACTGAGCCA
ISH Probe for CTGAGCCCAGGTATATATCTAACAGAAG EWSAT1		CTGAGCCCAGGTATATATCTAACAGAAG
ISH Probe for GGCTCAGTTCAGCAGGAA miR-24-3p		GGCTCAGTTCAGCAGGAA

to the hybridization solution and hybridized according to the manufacturer's protocol. After an incubation of slides with 4-nitroblue-tetrazolium for 30 minutes at 25°C and with nuclear fast red for 5 minutes at room temperature, the slices were observed and photographed under a microscope (Leica).

For the IHC assay, OS tissue specimens were fixed in 10% FBS at room temperature for 1 day and embedded in paraffin. Then, the embedded tissues were treated in order: paraffin-embedding, 4 µm thickness of the section, deparaffinization, rehydration, hydrogen peroxide incubation, antigen retrieval, 10% goat serum (BioWorld) blocking, first antibody incubation (Anti-ROCK1, Abcam) at 4°C overnight, secondary antibody incubation (Goat Anti-Rabbit IgG H&L, Abcam) at 37°C for 20 minutes, streptavidin-horseradish peroxidase complex incubation, diaminobenzidine tetrahydrochloride (MedChemExpress) stain, haematoxylin (Amresco) and counterstain. All sections were assessed by two experienced pathologists individually.

2.6 | Transwell assays

The procedure was conducted as previously described. ¹⁴ Briefly, OS cells were seeded on upper chambers (BD Bioscience). Culture medium with and without 10% FBS was supplemented into the lower and upper wells, respectively, and the entire set-up was incubated

for 24 hours. On the subsequent day, non-migrated cells were wiped out. Then, the filters were fixed in 90% ethanol, followed by crystal violet staining. Five random fields were counted per chamber using an inverted microscope (Olympus).

2.7 | Rhodamine phalloidin immunofluorescence

The actin filaments in OS cells were stained with rhodamine phalloidin as previously reported. Priefly, OS cells that reached 70-80% confluence were fixed in 4% formaldehyde for 10 minutes at room temperature and permeabilized with 0.3% Triton X-100 in PBS for 15 minutes. Then, the cells were incubated with 1 \times rhodamine phalloidin (Abcam) working solution at room temperature for 30 minutes and observed under a fluorescent microscope (Leica, Wetzlar, Germany). Images were analysed using Image-Pro Plus 6.0 software (Media Cybernetics).

2.8 | Western blot analysis

The procedure was conducted as previously described. Briefly, proteins were extracted with radioimmunoprecipitation assay lysis buffer (Sigma) and electrophoretically transferred onto PVDF membranes (Amresco). The membranes were incubated first with special primary antibodies that, respectively, probed ROCK1 (anti-ROCK1, Abcam, dilution rates of 1:2000), lysophosphatidic acid acyltransferase β (anti-LPAAT β , Abcam, concentration of 1 μ g/mL), and tyrosine kinase non-receptor 2 (anti-TNK2, Abcam, dilution rates of 1:50) at 4°C overnight and then with secondary antibodies (Abcam, dilution rates of 1:2000) at 25°C for 1 hour on the following day. Protein bands were detected on an X-ray film using an enhanced chemiluminescence detection system.

2.9 | Dual-luciferase reporter assay

Wild and mutant reporter plasmids that contain wild or mutant miR-24-3p binding sites, EWSAT1-wt and EWSAT1-mut and ROCK1-wt and ROCK1-mut, were synthesized by GenePharma. The procedure was performed as previously described. Briefly, when HEK293 cells achieved 70% confluence, EWSAT1-wt or ROCK1-wt and EWSAT1-mut or ROCK1-mut were co-transfected with miR-24-3p mimics and mimic control using Lipofectamine 3000 (Invitrogen), respectively. After 48 hours, luminescence changes in each group were determined using a Dual-Luciferase Reporter Assay System (Promega) according to the manufacturer's protocol.

2.10 | RNA pull-down assay

The procedure was conducted as previously described. ¹⁹ LncRNA-EWSAT1-wt and lncRNA-EWSAT1-wt were transcribed from vector pGEM®-T (Promega) and biotin-labelled with the Biotin RNA Labeling Mix (Roche, Basel, Switzerland) and T7 RNA polymerase

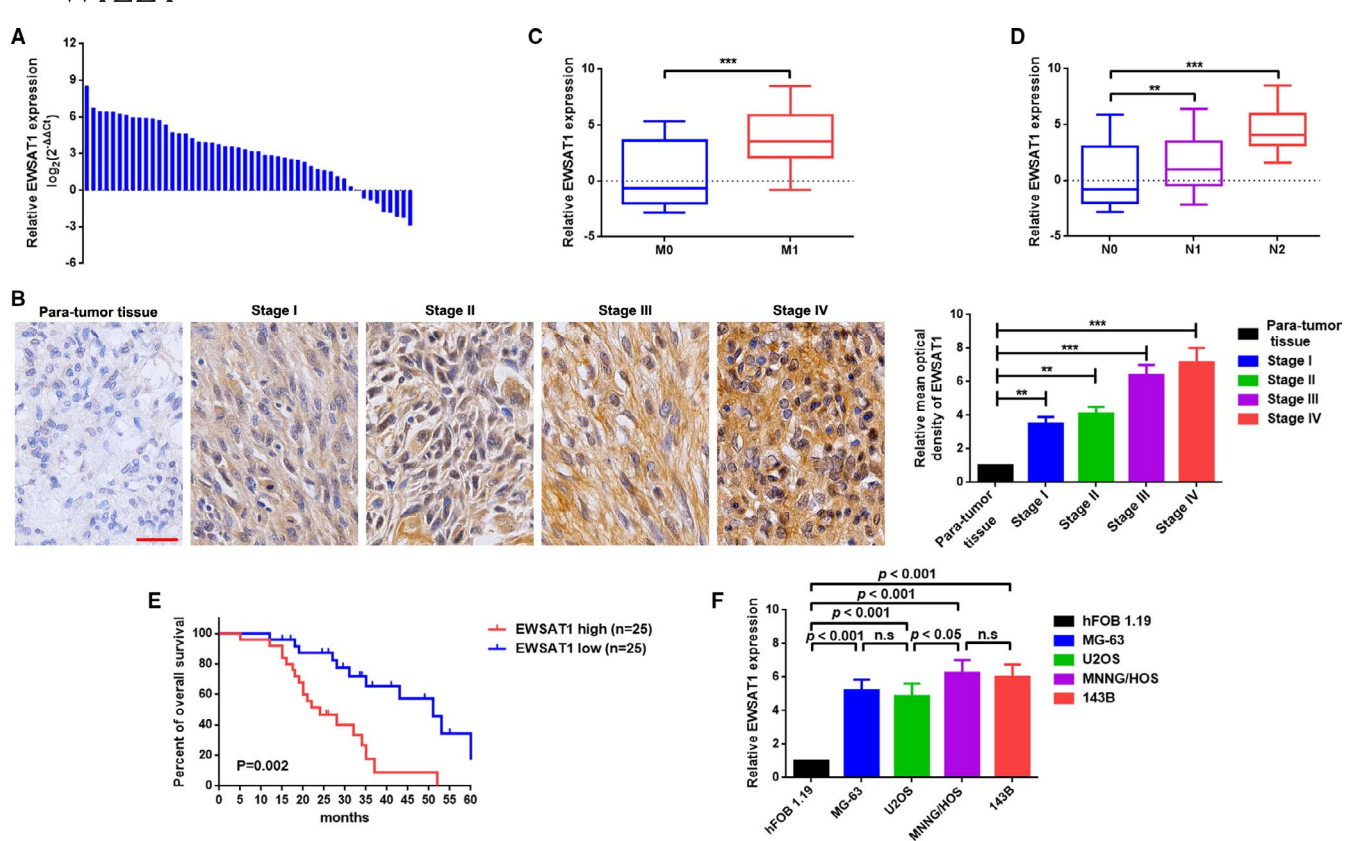


FIGURE 1 Elevated EWSAT1 was correlated with poor prognosis in patients with osteosarcoma (OS). A, Expression of EWSAT1 in OS tissue specimens was determined by qRT-PCR assay; data are shown as $^{\triangle}$ Ct. B, EWSAT1 was significantly elevated in patients with advanced staging as determined by in situ hybridization assay. **P < .001 when normalized and compared with the paratumour tissue group. C,D, EWSAT1 expression was remarkably elevated in patients with distant metastasis (C) and lymph node metastasis (D). **P < .01, **P < .001, when normalized and compared with the M $_0$ or N $_0$ group, respectively. E, Kaplan-Meier analyses indicated that the overall survival of patients with high EWSAT1 expression was significantly shorter than that of patients with low EWSAT1 expression, P = .002. F, EWSAT1 expression was elevated in the OS cell lines MG-63, U2OS, MNNG/HOS and 143B as determined by the qRT-PCR assay. P-values are shown in the diagram, and n.s. means non-significant. Data are shown as mean \pm SD from three independent experiments

(Roche), treated with RNase-free DNase I (Roche), and purified using an RNeasy Mini Kit (Qiagen). The biotinylated EWSAT1 probes were dissolved in binding and washing buffer and incubated with Dynabeads M-280 Streptavidin (Invitrogen) at 25°C for 10 minutes to generate probe-coated beads according to the manufacturer's protocol. Then, cell lysates of MNNG/HOS and 143B were incubated with probe-coated beads, and the RNA complexes bound to these beads were eluted and extracted for qRT-PCR analysis to detect the relative expression of miRNAs.

2.11 | Xenograft nude mouse model

Six-week-old female BALB/c nude mice were purchased from the Animal Care and Use Committee of Dalian Medical University Ltd. and maintained under sterile-specific pathogen-free conditions. Moreover, 200 μ L PBS containing 1 \times 10⁶ MNNG/HOS cells with stable overexpressed EWSAT1 or control vector (pMSCV) were intravenously injected into nude mice (n = 6 per group) for the evaluation of lung metastasis. The lungs of each group were harvested

for further detection after 6 weeks. This study was performed in accordance with the Guide for the Care and Use of Laboratory Animals of the National Institutes of Health and approved by the Institute Research Medical Ethics Committee of Central Hospital Affiliated to Shenyang Medical College. All efforts were made to minimize animal suffering, reduce the number of animals used and utilize possible alternatives to in vivo techniques.

2.12 | Statistical analysis

All experiments were repeated in triplicate, and all data from three independent experiments were expressed as mean \pm SD. GraphPad Prism version 5.0 (GraphPad Software, Inc) software and SPSS 19.0 statistical software were used for conducting statistical analysis. Pearson's chi-square test or Fisher's exact test was used to analyse the correlation between EWSAT1 and clinicopathological features of patients with OS; furthermore, log-rank test was used for survival analysis using GraphPad Prism version 5.0. Differences in the two groups were analysed using Student's t

TABLE 2 Association of EWSAT1 expression with clinicopathological features of osteosarcoma

		EWSA	EWSAT1	
Features	No. of cases	High	Low	P- value ^a
Age at diagnosis				
<18	31	18	13	.605
≥18	19	14	5	
Gender				
Female	28	17	11	.768
Male	22	15	7	
Histological subtype				
Osteoblastic	10	6	4	.896
Chondroblastic	11	8	3	
Fibroblastic	12	7	5	
Mixed	17	11	6	
Clinical stage				
I+IIA	23	10	13	.008
IIB/III	27	22	5	
Distant metastasis				
Absent	21	9	12	.016
Present	29	23	6	
Tumour size (cm)				
<5	22	13	11	.239
≥5	28	19	7	
Anatomic location				
Tibia/femur	26	18	8	.557
Elsewhere	24	14	10	

^aP-value obtained from Pearson chi-square test or Fisher's exact test.

test or one-way analysis of variance. Differences were considered significant if P < .05.

3 | RESULTS

3.1 | EWSAT1 was elevated and correlated with poor prognosis in patients with OS

EWSAT1 expression in the collected OS tissue specimens was determined using qRT-PCR. As presented in Figure 1A, EWSAT1 had high expression in most (43/50, 86.00%) OS tissue specimens compared with that of paratumour tissue specimens. Additionally, ISH was applied to measure the expression of EWSAT1 in different stages of OS tissue specimens. As shown in Figure 1B, the expression of EWSAT1 gradually increased with advanced staging (P < .001). Further, we found that elevated EWSAT1 expression was more commonly present in OS tissue specimens with distant metastasis and lymph node metastasis (Figure 1C,D, P < .001). Furthermore, we analysed the correlation between EWSAT1 expression and clinicopathological

features of patients with OS. As shown in Figure 1E and Table 1, patients with OS were divided into the high- and low-EWSAT1 groups according to the expression using a median method. Moreover, high EWSAT1 expression was closely correlated with shorter survival rate (Figure 1E, P=.002), advanced staging (IIB/III) (P=.008) and distant metastasis (P=.016) (Table 2). Eventually, EWSAT1 expression in the normal human osteoblastic cell line hFOB 1.19 and the four OS cell lines MG-63, U2OS, HOS and 143B was determined using qRT-PCR. As shown in Figure 1F, EWSAT1 expression was significantly up-regulated in four OS cell lines compared with that in hFOB 1.19 (P<.001).

3.2 | Knockdown of EWSAT1 suppressed migration and induced actin stress fibres dissolution in MNNG/HOS and 143B cells

In the previous section, we elucidated that high EWSAT1 expression was closely related to distant metastasis and lymph node metastasis. Therefore, we attempted to explore the role of EWSAT1 in cell migration at the cellular level. We first knocked down the expression of EWSAT1 in MNNG/HOS and 143B cells in an RNAi experiment. As shown in Figure 2A,B, EWSAT1 was knocked down by transfection of EWSAT1 siRNA (compared with si-con, 1# si-EWSAT1 presented a higher silence efficacy and was selected as the silencing tool in the following RNAi experiments, P < .01). Second, Transwell assay was performed to evaluate the effect of EWSAT1 on OS cell migration. As presented in Figure 2C, knockdown of EWSAT1 suppressed cell migration in MNNG/HOS and 143B cells (P < .01). Epithelial-tomesenchymal transition (EMT) is extensively reported as a key process in cancer cell metastasis.²⁰ Consequently, we determined the role of EWSAT1 in OS cell EMT. As presented in Figure 2D,E, knockdown of EWSAT1 suppressed N-cadherin but promoted E-cadherin expression.

Reorganization of actin cytoskeleton is the initial power of cell motility and is essential for the migration of most cancer cells. Accordingly, we detected the effect of EWSAT1 on actin cytoskeleton changes. As presented in Figure 2F, knockdown of EWSAT1 also induced dissolution of actin stress fibres (P < .01).

3.3 | EWSAT1 promoted migration and actin stress fibre formation by up-regulation of ROCK1 in MNNG/ HOS and 143B cells

Our study and other previous studies demonstrated that ROCK1 was a key molecule in migration and actin stress fibre formation in OS cells. Here, we attempted to explore whether ROCK1 was a downstream effector of EWSAT1. By analysing GEO datasets GSE87437, we first displayed that the expression of ROCK1 was positively correlated with EWSAT1 (Figure 3A). Second, we revealed that an elevation or depression of EWSAT1 positively

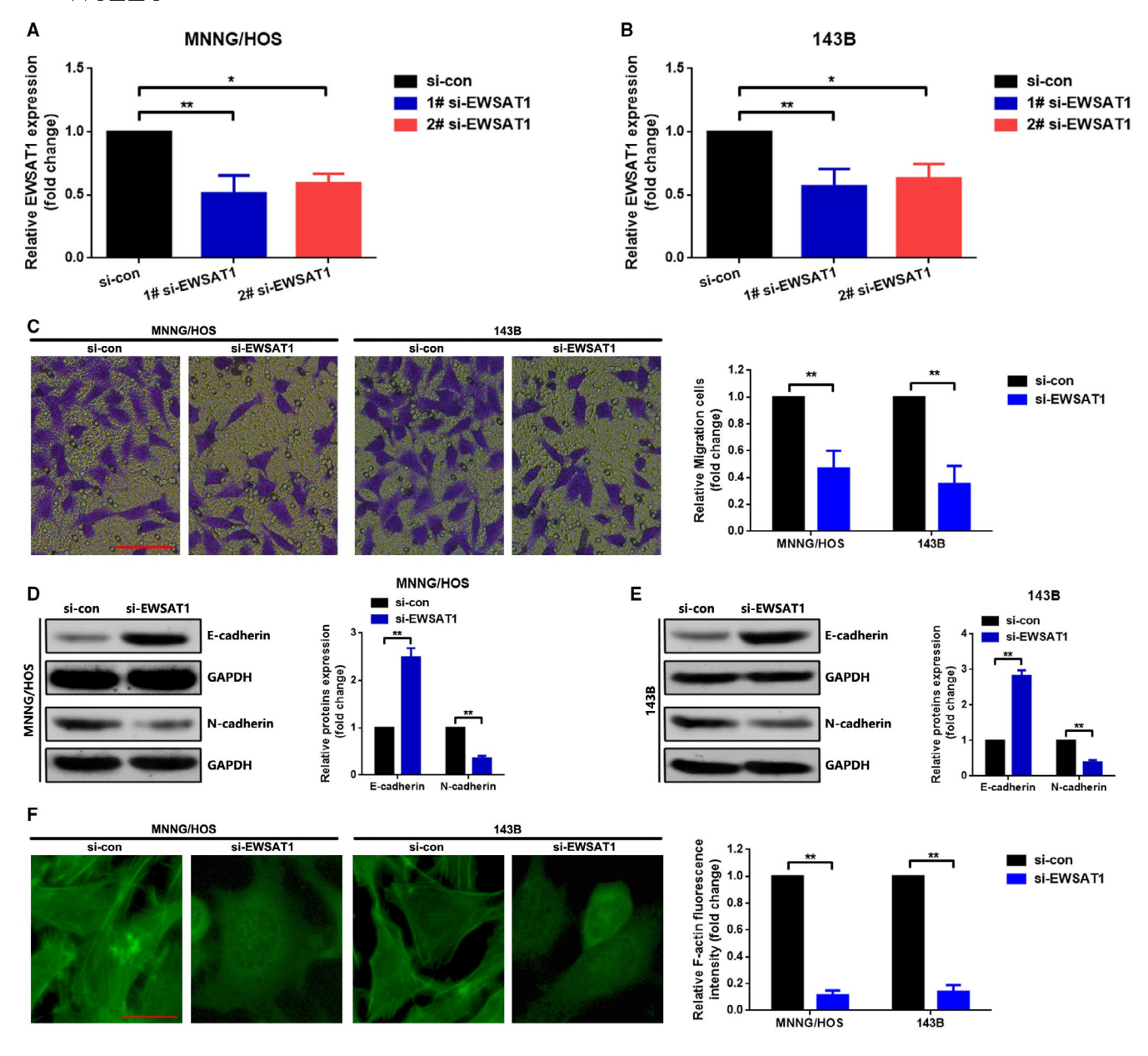


FIGURE 2 Knockdown of EWSAT1 suppressed migration and induced actin stress fibre dissolution in MNNG/HOS and 143B cells. A,B, EWSAT1 was knocked down in MNNG/HOS (A) and 143B (B) cells as confirmed by qRT-PCR assay. C, Down-regulation of EWSAT1 suppressed the migration of osteosarcoma (OS) cells as determined from the Transwell assay. D,E, Expression of E-cadherin and N-cadherin was determined by Western blot assay. F, Knockdown of EWSAT1 induced the dissolution of actin stress fibres in OS cells as determined from rhodamine phalloidin immunofluorescence. $^*P < .05$ and $^{**P} < .01$ when normalized and compared with the si-con group, respectively. Data are shown as mean \pm SD from three independent experiments

regulated ROCK1 expression at the protein level but not at the mRNA level (Figure 3B-D, P < .01). Third, Y-27632 dihydrochloride—a selective ROCK1 inhibitor—was applied to investigate the potential role of ROCK1 played in EWSAT1 in promoting OS cell migration and actin stress fibre formation. As presented in Figure 3D,E, Y-27632 dihydrochloride dramatically attenuated EWSAT1-induced migration and actin stress fibre formation in MNNG/HOS and 143B cells (P < .01). Briefly, the outcomes of this section showed that EWSAT1 up-regulated the expression of the ROCK1 protein to promote migration and actin stress fibre formation in MNNG/HOS and 143B cells.

3.4 | EWSAT1 up-regulated ROCK1 through sponging of miR-24-3p

It is well known that IncRNAs could regulate their target genes through a mechanism involving ceRNA. We focused on whether any miRNAs might serve as a bridge between EWSAT1 and ROCK1. Through an online prediction, miR-24-3p was viewed for its similar MREs for both EWSAT1 and ROCK1 (Figure 4A). Then, through a luciferase assay, we verified that EWSAT1 and ROCK1 were both targeted by miR-24-3p through similar miR-24-3p response elements (MREs-24-3p) (Figure 4B). Further, we elucidated that EWSAT1 and

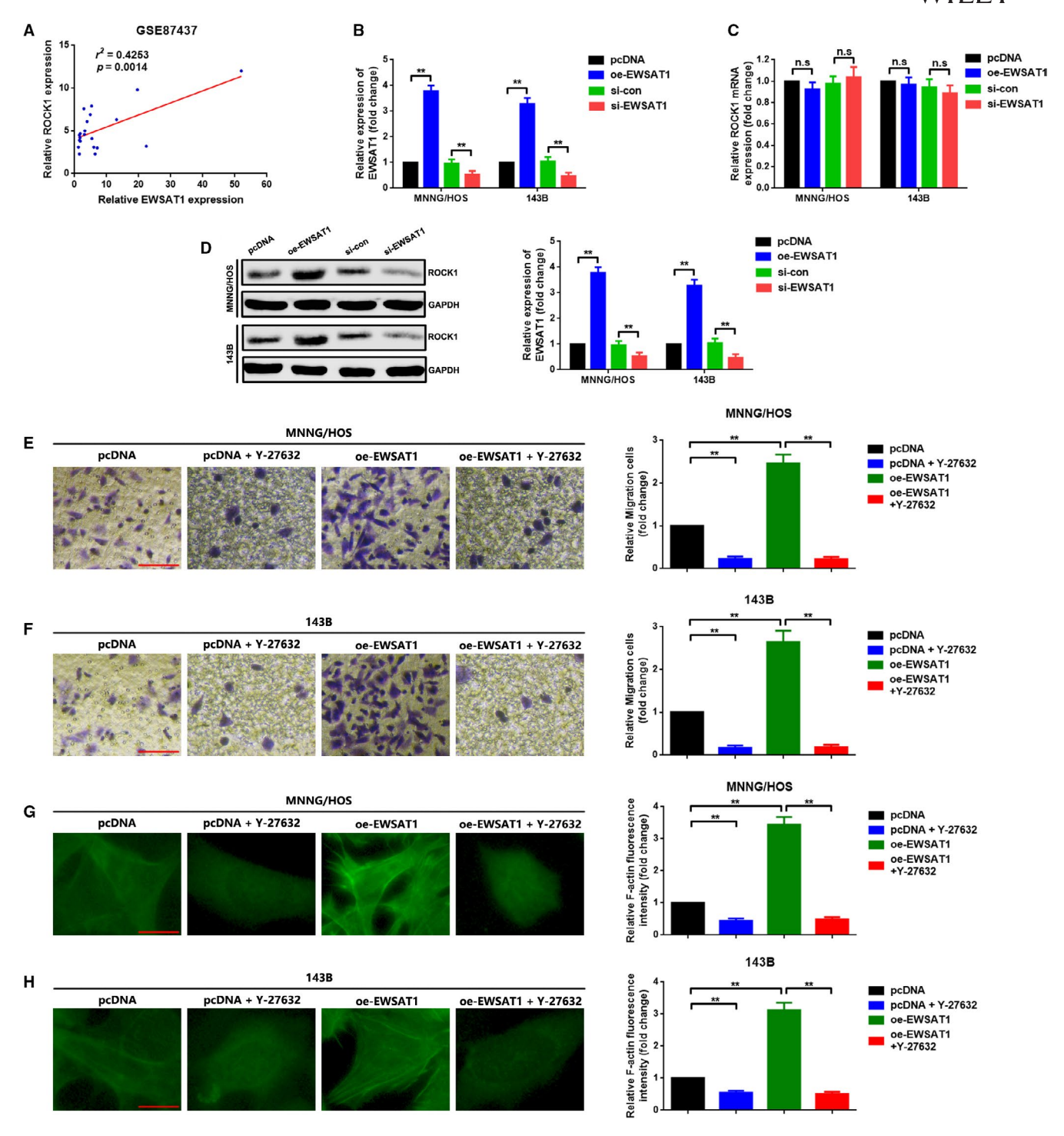


FIGURE 3 A, The relationship between ROCK1 and EWSAT1 in GEO data sets 87437 was determined by Spearman correlation analysis, $r^2 = .4253$, P = .0014. B, Expression of EWSAT1 after transfection of oeEWSAT1 and si-EWSAT1 was confirmed using qRT-PCR assay. **P < 0.01 when normalized with the pcDNA group and compared with the pcDNA and si-con groups, individually. C, Up- and down-regulation of EWSAT1 presented no effect on ROCK1 mRNA expression, which were confirmed using qRT-PCR assay. **P < .01 when normalized with the pcDNA group and compared with the pcDNA and si-con groups, individually. D, ROCK1 protein expression was positively regulated by EWSAT1 as determined using the Western blot assay. **P < .01 when normalized with the pcDNA group and compared with the pcDNA and si-con groups, respectively. E,F, The migration ability of osteosarcoma (OS) cells was significantly enhanced by transfection of oe-EWSAT1, while the facilitative effect was remarkably attenuated using Y-27632 dihydrochloride—the selective ROCK1 blocker. G,H, Overexpression of EWSAT1 promoted actin stress fibre formation, but the facilitative effect was reversed using Y-27632 dihydrochloride. **P < .01 when normalized with the pcDNA group and compared with the oe-EWSAT1 group. Data are shown as mean \pm SD from three independent experiments

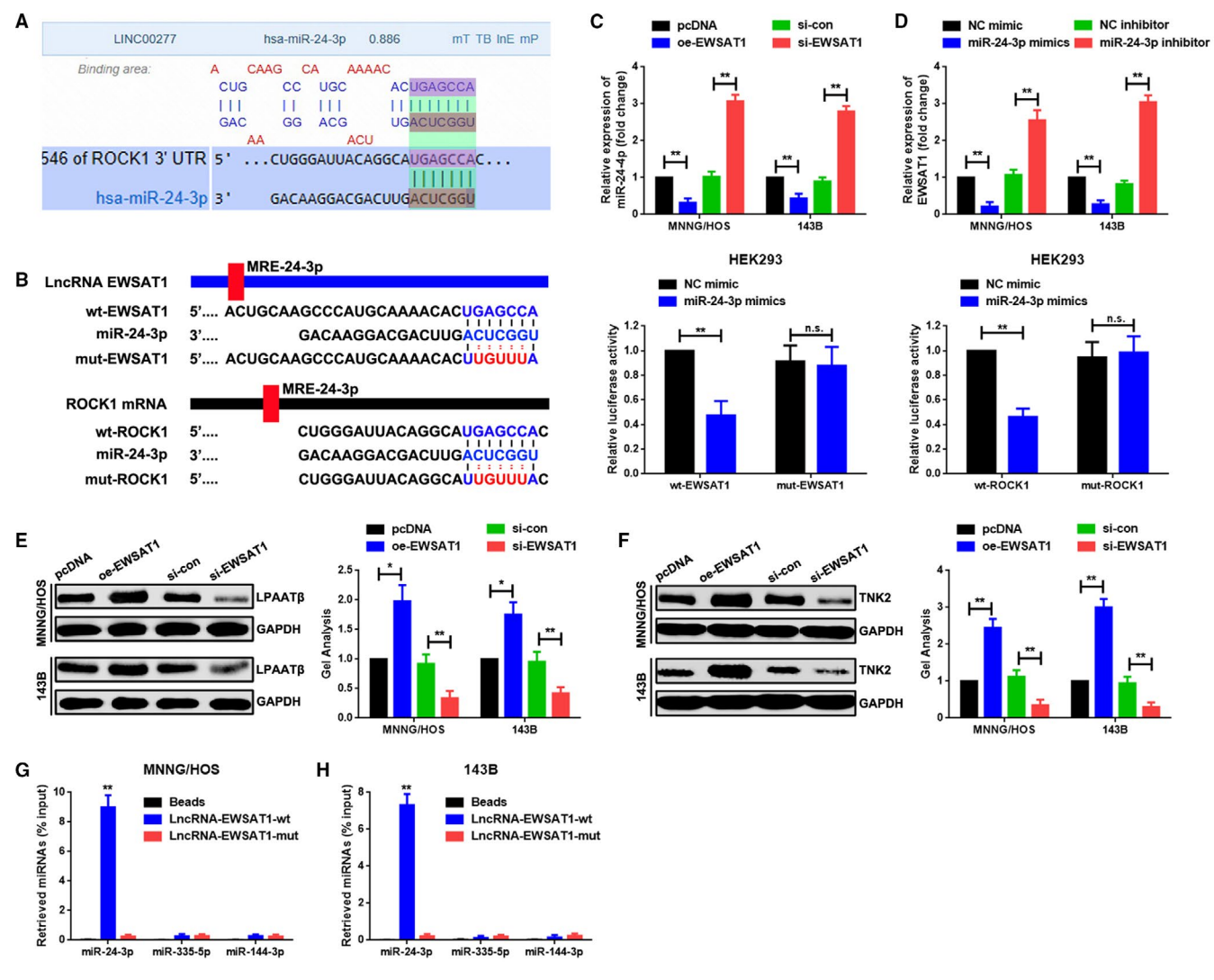


FIGURE 4 EWSAT1 up-regulated ROCK1 through the sponging of miR-24-3p. A, EWSAT1 and ROCK1 shared similar MREs for miR-24-3p as predicted online using DIANA-LncBase (http://carolina.imis.athena-innovation.gr) and Targetscan (http://www.targetscan.org/vert_71). B, Dural luciferase assay demonstrated that it was a cotransfection of miR-24-3p mimics and wt-EWSAT1/wt-ROCK1 rather than a cotransfection of miR-24-3p mimics and mut-EWSAT1/mut-ROCK1 that led to an evident weakening of luminescence. **P < .01, n.s. P > .05 when normalized and compared with the mimic control group. C,D, EWSAT1 and miR-24-3p regulated each other in a reciprocal manner. **P < .01 when normalized and compared with the pcDNA and NC mimic groups, individually. E,F, Up- and down-regulation of EWSAT1 positively regulated LPAATβ and TNK2 expression at the protein level as determined using Western blot assay. *P < .05, **P < .01 when normalized and compared with the pcDNA group. G,H, Cell lysates collected from MNNG/HOS and 143B cells were incubated with biotin-labelled lncRNA-EWSAT1-wt and lncRNA-EWSAT1-mut individually. It was lncRNA-EWSAT1-wt rather than lncRNA-EWSAT1-mut that could pull down miR-24-3p. However, neither miR-335-5p nor miR-144-3p was pulled down by any of the two plasmids (lncRNA-EWSAT1-wt and lncRNA-EWSAT1-mut). **P < .01 when normalized and compared with the beads group. Data are shown as mean \pm SD from three independent experiments

miR-24-3p affected each other's expression in a reciprocal manner (Figure 4C,D, P < .01). Furthermore, we illustrated that an elevation or depression in EWSAT1 expression regulated not only ROCK1 (Figure 3A,B, P < .01) but also LPAAT β and TNK2^{22,23}—two other verified downstream targeted genes of miR-24-3p (Figure 4E,F, P < .01). Lastly, through a RNA pull-down assay, we demonstrated that biotin-labelled lncRNA-EWSAT1-wt (containing wild MREs-24-3p) rather than lncRNA-EWSAT1-mut (containing mutant MREs-24-3p)

precipitated miR-24-3p, which again proved the binding effect between EWSAT1 and miR-24-3p. More convincingly, the results of the RNA pull-down assay also indicated that neither lncRNA-EWSAT1-wt nor lncRNA-EWSAT1-mut pulled down miR-335-5p and miR-144-3p—two previously verified miRNAs that targeted ROCK1 (Figure 4G,H, P < .01). Generally, the above-mentioned data demonstrated strongly that EWSAT1 promoted ROCK1 through sponging of miR-24-3p.

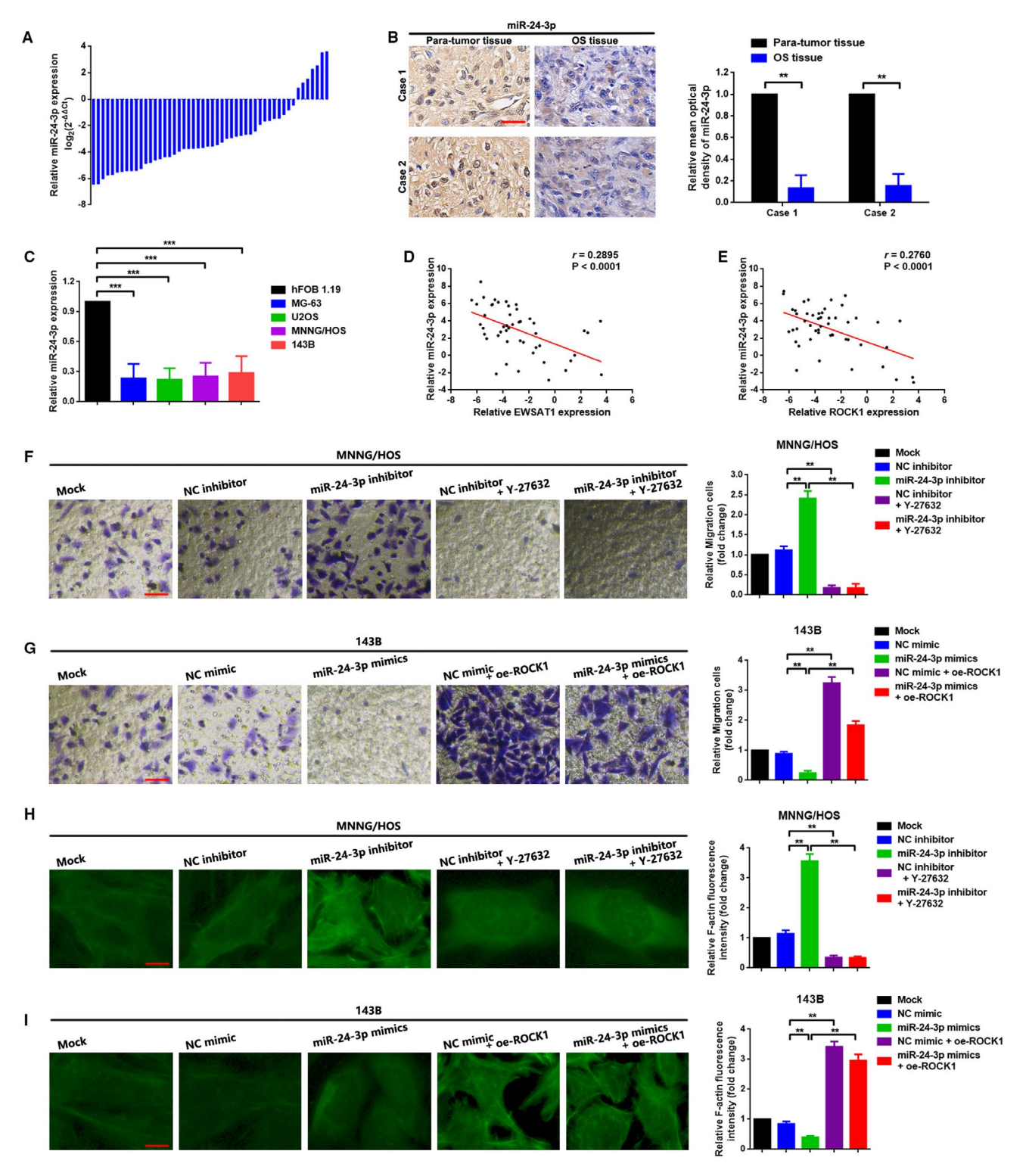


FIGURE 5 A,B, MiR-24-3p expression in osteosarcoma (OS) tissue specimens was measured using the qRT-PCR assay (data are shown as \triangle Ct) and in situ hybridization assay. **P < .01 when normalized and compared with the paratumor tissue group. C, MiR-24-3p expression was down-regulated in the OS cell lines MG-63, U2OS, MNNG/HOS and 143B as determined by the qRT-PCR assay. ***P < .001 when normalized and compared with the hFOB1.19 group. D, A negative correlation between EWSAT1 and miR-24-3p was confirmed by Pearson correlation analysis, P < .0001. E, The same tendency was observed between ROCK1 and miR-24-3p as shown using Pearson correlation analysis, P < .0001. F,G,H,I, Knock-down of miR-24-3p promoted OS cell migration and actin stress fibre formation, while the facilitative effect could be reversed using Y-27632 dihydrochloride. On the contrary, up-regulation of miR-24-3p inhibited OS cell migration and actin stress fibre formation, while the suppressive effect was reversed using the ROCK1 overexpression plasmid oe-ROCK1. **P < .01 when normalized with the Mock group and compared with the miR-24-3p inhibitor group or the miR-24-3p mimics group, separately. Data are shown as mean \pm SD from three independent experiments

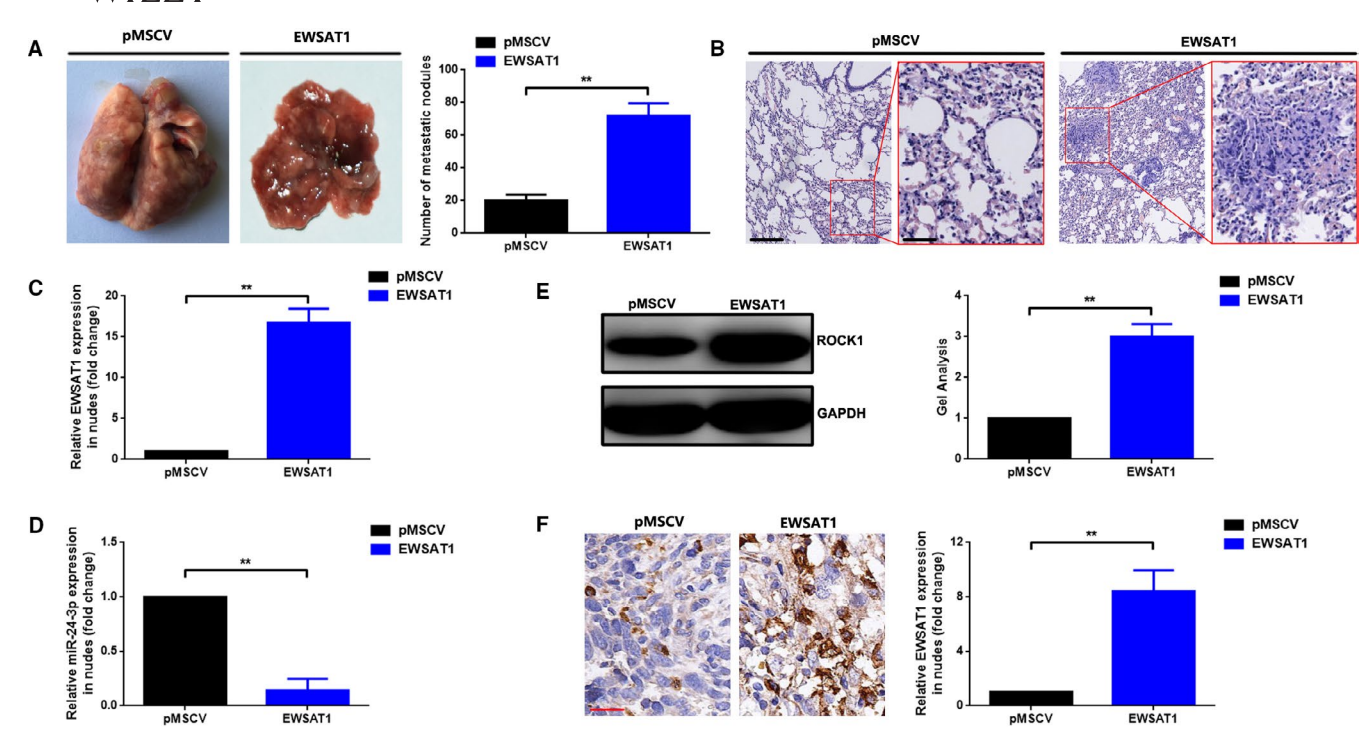


FIGURE 6 EWSAT1 promoted lung metastasis of osteosarcoma (OS) in vivo. A, Representative photos of the metastatic nodules in the lungs. B, Overexpression of EWSAT1 promoted lung metastasis of OS as presented by the representative haematoxylin-eosin (HE) staining (scale bar of 200 μ m for a magnification of 100 \times and scale bar of 50 μ m for a magnification of 400 \times , respectively). C, EWSAT1 expression in the metastatic nodules was qualified using the qRT-PCR assay. D, MiR-24-3p expression in the metastatic nodules was also measured using the qRT-PCR assay. E,F, Expression of the ROCK1 protein in the metastatic nodules was determined using the Western blot assay (E) and IHC assay (F), respectively. **P < .01 when normalized and compared with the pMSCV group. Data are shown as mean \pm SD from three independent experiments

3.5 | MiR-24-3p suppressed ROCK1-mediated migration and actin stress fibre formation in MNNG/ HOS and 143B cells

In this section, we focused on the function of miR-24-3p working on OS cell migration and actin stress fibre formation. First, we observed that miR-24-3p was down-regulated in OS tissue specimens and cell lines (Figure 5A-C). Second, we elucidated negative correlations between miR-24-3p and ROCK1, miR-24-3p, and EWSAT1 (Figure 5D,E, P < .0001). Lastly, we demonstrated that depression in miR-24-3p expression promoted migration and actin stress fibre formation, while the facilitative effect could be reversed by Y-27632 dihydrochloride (Figure 5F,G, P < .01). Thus, combined with the targeted binding effect between miR-24-3p and ROCK1 3'-UTR (Figure 4B), the outcomes of this section indicated that miR-24-3p was an upstream regulator of ROCK1 and its mediated migration and actin stress fibre formation.

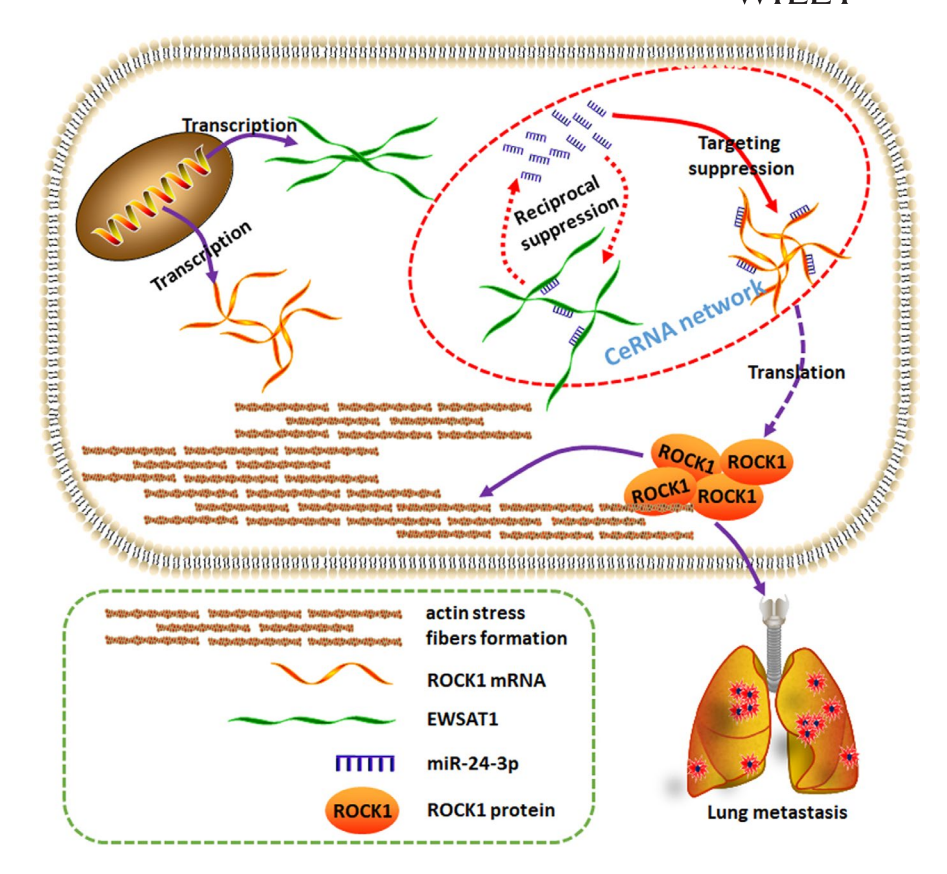
3.6 | EWSAT1 promoted lung metastasis of OS in vivo

In this section, xenograft mouse models were constructed to verify the function of EWSAT1 in OS in vivo. MNNG/HOS cells with stably overexpressing EWSAT1 and with corresponding vector were inoculated intravenously to the mice. As shown in Figure 6A,B (P < .01), the number of microscopic metastatic tumour nodules in the lungs in the EWSAT1 group was significantly higher than that in the pMSCV group. We further detected the expression of EWSAT1, miR-24-3p and ROCK1 in each group. As presented in Figure 6C-F, up-regulated EWSAT1 and ROCK1 expression but down-regulated miR-24-3p expression were found in the EWSAT1 group compared with those in the pMSCV group (P < .01).

4 | DISCUSSION

Increasing evidence suggests that non-coding RNAs, including IncR-NAs, miRNAs and circular RNAs (circRNAs), comprehensively participate in diverse diseases and cellular processes. $^{24-26}$ EWSAT1, which contains four exons, is located at human chromosome 15q23 and reported as an oncogene in several cancers including ovarian cancer, nasopharyngeal carcinoma, Ewing sarcoma and OS. $^{8,9,27-29}$ In the present study, we observed that EWSAT1 expression was upregulated in the OS tissue and that a higher EWSAT1 was correlated with shorter survival rate (P = .002), higher advanced TNM staging (P = .008) and rapid distant metastasis (P = .016). Moreover, through loss-of-function experiments, we verified that EWSAT1 promoted migration and actin stress fibre formation in two OS cell lines: MNNG/HOS and 143B. Furthermore, through an in vivo animal

FIGURE 7 Schematic diagram of the mechanism. LncRNA EWSAT1 promoted metastasis and actin cytoskeleton changes through miR-24-3p sponging in osteosarcoma (OS)



study, we demonstrated that overexpression of EWSAT1 promoted lung metastasis of OS. Therefore, we thought that EWSAT1 would act as a tumour initiator in OS, especially in OS metastasis.

Cancer cell metastasis is a multistage process involving invasion into the surrounding tissue, intravasation, transit into the blood or lymph, extravasation and growth at a new site.³⁰ Cell migration, which has a fundamental role in tumour invasion and metastasis, is a very complicated issue, and reorganization of the actin cytoskeleton produces the necessary force for cell migration. ²¹ The actin cytoskeleton plays a critical role in tumour cell migration and movement.³¹ Cai reported that ectopic expression of miR-23a promoted dissolution of actin stress fibres in PC-3 and DU145 cells.³² It is well uncovered that some classical signalling pathways, including ras homolog family (Rho) and ROCK signalling pathway, play a vital regulative effect in cytoskeletal reorganization. 33-35 Cai found that knockdown of lncRNA MALAT1 reduced the number of actin stress fibres and suppressed metastasis through the down-regulation of ROCK1 in the OS cell.¹⁷ In our previous studies, we also demonstrated that ROCK1 was a key molecule in OS cell metastasis. 12,13,15,36,37 In the present study, we illustrated that blockage of ROCK1 significantly impaired EWSAT1induced migration and cytoskeletal changes, and this phenomenon indicated that ROCK1 was a substrate of EWSAT1 in OS cells.

miRNAs are another type of non-coding RNAs that are 22-25 nt in length. MiRNAs play critical roles in various cell biological behaviours, including proliferation, apoptosis, cell cycle control, cell differentiation and metastasis. ³⁸⁻⁴⁰ As a member of the miRNA family, miR-24-3p (also known as miR-24) is extensively involved in oncogenesis and

progression of multiple cancers, including OS. Liu found that miR-24-3p significantly suppressed OS cell metastasis mediated by inhibiting Ack1 expression.²² Through in vitro and in vivo studies, Song reported that miR-24-3p inhibited OS cell proliferation by targeting LPAATβ. ²³ In the present study, we also found that miR-24-3p was down-regulated and served as a bridge between EWSAT1 and ROCK1 in OS. Through luciferase assay and RNA pull-down assay, we illustrated that miR-24-3p regulated EWSAT1 and ROCK1 expression by direct targeting. Functionally, miR-24-3p is involved in ROCK1-mediated metastasis and cytoskeletal changes. Recently, a prevalent theory on IncRNA, miRNA and mRNA is the ceRNA theory. The CeRNA hypothesis is that all types of RNA transcripts could undergo cross-talk through a new "language" mediated by similar MREs. Through a series of qRT-PCRs, we clarified the reciprocal effect between EWSAT1 and miR-24-3p. Further, we showed that EWSAT1 positively regulated ROCK1, LPAATB and TNK2, three downstream targets of miR-24-3p. Moreover, through the RNA pull-down assay, we demonstrated that IncRNA-EWSAT1-wt pulled down only miR-24-3p but not miR-335-5p and miR-144-3p-two previously verified miRNAs that targeted ROCK1. These results strongly demonstrated that EWSAT1 served as a ceRNA of ROCK1 through sponging of miR-24-3p.

5 | CONCLUSION

Generally, as presented in Figure 7, all results of our study illustrated that EWSAT1 regulated ROCK1 and mediated migration and actin

cytoskeletal changes through miR-24-3p decoying. Our present study proposed a new targeted axial in the treatment of OS.

ACKNOWLEDGEMENTS

This work was supported by SMC General Science Foundation (grant No. 20182034), Youth Talent Support Program of Liaoning Province (grant No. XLYC1907011), SMC Students' scientific research projects (grant No. 20189021), Key R&D Program of Liaoning Province (grants No. 2018225014), Higher Institute Program Foundation for the Innovative Talents of Liaoning Province (grant No. LR2017056), Technological innovation fund of Shenyang Technology Division (grant No. RC190008 and 19-112-4-023) and National Natural Science Foundation of China (grant No. 81972522 and 81502333).

CONFLICT OF INTEREST

The authors declare no conflicts of interest.

AUTHOR CONTRIBUTION

Dewei Shen: Investigation (equal). Yize Liu: Investigation (equal). Yuexin Liu: Investigation (equal). Tao Wang: Investigation (supporting). Lin Yuan: Investigation (supporting). Xuyang Huang: Investigation (supporting). Yong Wang: Data curation (equal); Funding acquisition (equal); Software (equal); Supervision (equal); Writing-original draft (equal); Writing-review & editing (equal).

DATA AVAILABILITY STATEMENT

The data used to support the findings of this study are available from the corresponding author upon request.

ORCID

Yong Wang https://orcid.org/0000-0003-3674-9403

REFERENCES

- Ottaviani G, Jaffe N. The epidemiology of osteosarcoma. Cancer Treat Res. 2009;152:3-13.
- Berner K, Johannesen TB, Berner A, et al. Time-trends on incidence and survival in a nationwide and unselected cohort of patients with skeletal osteosarcoma. Acta Oncologica. 2015;54:25-33.
- Hung GY, Yen HJ, Yen CC, et al. Improvement in high-grade osteosarcoma survival: results from 202 patients treated at a single institution in Taiwan. Medicine. 2016;95:e3420.
- Sampo M, Koivikko M, Taskinen M, et al. Incidence, epidemiology and treatment results of osteosarcoma in Finland - a nationwide population-based study. Acta Oncologica. 2011;50:1206-1214.
- Chen ZZ, Huang L, Wu YH, Zhai WJ, Zhu PP, Gao YF. LncSox4 promotes the self-renewal of liver tumour-initiating cells through Stat3-mediated Sox4 expression. *Nat Commun*. 2016;7:12598.
- Li D, Liu X, Zhou J, et al. Long noncoding RNA HULC modulates the phosphorylation of YB-1 through serving as a scaffold of extracellular signal-regulated kinase and YB-1 to enhance hepatocarcinogenesis. Hepatology. 2017;65:1612-1627.
- 7. Orom UA, Shiekhattar R. Long noncoding RNAs usher in a new era in the biology of enhancers. *Cell.* 2013;154:1190-1193.
- Marques Howarth M, Simpson D, Ngok SP, et al. Long noncoding RNA EWSAT1-mediated gene repression facilitates Ewing sarcoma oncogenesis. J Clin Investig. 2014;124:5275-5290.

- Sun L, Yang C, Xu J, Feng Y, Wang L, Cui T. Long noncoding RNA EWSAT1 promotes osteosarcoma cell growth and metastasis through suppression of MEG3 expression. DNA Cell Biol. 2016;35:812-818.
- Salmena L, Poliseno L, Tay Y, Kats L, Pandolfi PP. A ceRNA hypothesis: the Rosetta Stone of a hidden RNA language? *Cell*. 2011;146:353-358.
- Liu Y, Wang Y, Fu X, Lu Z. Long non-coding RNA NEAT1 promoted ovarian cancer cells' metastasis through regulation of miR-382-3p/ ROCK1 axial. *Cancer Sci.* 2018;109:2188-2198.
- Wang Y, Lu Z, Wang N, et al. Long noncoding RNA DANCR promotes colorectal cancer proliferation and metastasis via miR-577 sponging. Exp Mol Med. 2018;50:57.
- Wang Y, Yang T, Zhang Z, et al. Long non-coding RNA TUG1 promotes migration and invasion by acting as a ceRNA of miR-335-5p in osteosarcoma cells. Cancer Sci. 2017;108:859-867.
- Wang Y, Zeng X, Wang N, et al. Long noncoding RNA DANCR, working as a competitive endogenous RNA, promotes ROCK1mediated proliferation and metastasis via decoying of miR-335-5p and miR-1972 in osteosarcoma. Mol Cancer. 2018;17:89.
- Wang Y, Zhang Y, Yang T, et al. Long non-coding RNA MALAT1 for promoting metastasis and proliferation by acting as a ceRNA of miR-144-3p in osteosarcoma cells. *Oncotarget*. 2017;8:59417-59434.
- Zhou X, Hu M, Ge Z. Tumorsuppressive miR2993p inhibits gastric cancer cell invasion by targeting heparanase. Mol Med Rep. 2019;20:2151-2158.
- 17. Cai X, Liu Y, Yang W, et al. Long noncoding RNA MALAT1 as a potential therapeutic target in osteosarcoma. *J Orthop Res.* 2016;34:932-941.
- 18. Wang K, Jin W, Song Y, Fei X. LncRNA RP11-436H11.5, functioning as a competitive endogenous RNA, upregulates BCL-W expression by sponging miR-335-5p and promotes proliferation and invasion in renal cell carcinoma. *Mol Cancer.* 2017;16:166.
- Song YX, Sun JX, Zhao JH, et al. Non-coding RNAs participate in the regulatory network of CLDN4 via ceRNA mediated miRNA evasion. Nat Commun. 2017;8:289.
- 20. Savagner P. The epithelial-mesenchymal transition (EMT) phenomenon. *Ann Oncol.* 2010;21 Suppl 7:vii89-92.
- Yamazaki D, Kurisu S, Takenawa T. Regulation of cancer cell motility through actin reorganization. Cancer Sci. 2005;96:379-386.
- 22. Liu Z, Liu Z, Zhang Y, Li Y, Liu B, Zhang K. miR-24 represses metastasis of human osteosarcoma cells by targeting Ack1 via AKT/MMPs pathway. *Biochem Biophys Res Comm.* 2017;486:211-217.
- Song L, Yang J, Duan P, et al. MicroRNA-24 inhibits osteosarcoma cell proliferation both in vitro and in vivo by targeting LPAATbeta. Arch Biochem Biophys. 2013;535:128-135.
- 24. Hesse M, Arenz C. MicroRNA maturation and human disease. *Methods Mol Biol.* 2014;1095:11-25.
- 25. Kazemzadeh M, Safaralizadeh R, Orang AV. LncRNAs: emerging players in gene regulation and disease pathogenesis. *J Genet*. 2015;94:771-784.
- 26. Qu S, Yang X, Li X, et al. Circular RNA: a new star of noncoding RNAs. *Cancer Lett.* 2015;365:141-148.
- 27. Fu X, Zhang L, Dan L, Wang K, Xu Y. LncRNA EWSAT1 promotes ovarian cancer progression through targeting miR-330-5p expression. *Am J Transl Res.* 2017;9:4094-4103.
- Song P, Yin SC. Long non-coding RNA EWSAT1 promotes human nasopharyngeal carcinoma cell growth in vitro by targeting miR-326/-330-5p. Aging. 2016;8:2948-2960.
- 29. Zhang GY, Zhang JF, Hu XM, Luo ZP, Ma YZ. Clinical significance of long non-coding RNA EWSAT1 as a novel prognostic biomarker in osteosarcoma. *Eur Rev Med Pharmacol Sci.* 2017;21:5337-5341.
- Olson MF, Sahai E. The actin cytoskeleton in cancer cell motility. Clin Exp Metas. 2009;26:273-287.

- O'Neill GM. The coordination between actin filaments and adhesion in mesenchymal migration. Cell Adh Migr. 2009;3:355-357.
- 32. Cai S, Chen R, Li X, et al. Downregulation of microRNA-23a suppresses prostate cancer metastasis by targeting the PAK6-LIMK1 signaling pathway. *Oncotarget*. 2015;6:3904-3917.
- Oh KS, Oh BK, Park CH, Mun J, Won SH, Lee BH. Baicalein potently inhibits Rho kinase activity and suppresses actin stress fiber formation in angiotensin II-stimulated H9c2 cells. *Biol Pharm Bull*. 2012;35:1281-1286.
- 34. Schofield AV, Bernard O. Rho-associated coiled-coil kinase (ROCK) signaling and disease. *Crit Rev Biochem Mol Biol.* 2013;48:301-316.
- Sun J, Zhang D, Zheng Y, et al. Targeting the metastasis suppressor, NDRG1, using novel iron chelators: regulation of stress fiber-mediated tumor cell migration via modulation of the ROCK1/pMLC2 signaling pathway. Mol Pharmacol. 2013;83:454-469.
- Wang Y, Wang N, Zeng X, et al. MicroRNA-335 and its target Rock1 synergistically influence tumor progression and prognosis in osteosarcoma. *Oncol Lett.* 2017;13:3057-3065.

- Wang Y, Zhao W, Fu Q. miR-335 suppresses migration and invasion by targeting ROCK1 in osteosarcoma cells. Mol Cell Biochem. 2013;384:105-111.
- 38. Abba M, Patil N, Allgayer H. MicroRNAs in the regulation of MMPs and metastasis. *Cancers*. 2014;6:625-645.
- Garofalo M, Croce CM. MicroRNAs: master regulators as potential therapeutics in cancer. Annu Rev Pharmacol Toxicol. 2011;51:25-43.
- 40. Lee YS, Dutta A. MicroRNAs in cancer. Annu Rev Pathol. 2009;4:199-227.

How to cite this article: Shen D, Liu Y, Liu Y, et al. Long non-coding RNA EWSAT1 promoted metastasis and actin cytoskeleton changes via miR-24-3p sponging in osteosarcoma. *J Cell Mol Med.* 2020;00:1–13. https://doi.org/10.1111/jcmm.16121